Solution Structure of Co·Bleomycin A2 Green Complexed with d(CCAGGCCTGG)

Wei Wu,[†,||] Dana E. Vanderwall,[‡,||] Christopher J. Turner,*[,§] John W. Kozarich,*[,‡,⊥] and JoAnne Stubbe*[,†]

Contribution from the Departments of Chemistry and Biology, Massachusetts Institute of Technology, Cambridge, Massachusetts 02139, Department of Chemistry and Biochemistry, University of Maryland, College Park, Maryland 20742, and Francis Bitter Magnet Laboratory, Massachusetts Institute of Technology, Cambridge, Massachusetts 02139

Received July 25, 1995[⊗]

Abstract: The solution structure of Co·Bleomycin (CoBLM) A2 green (the hydroperoxide form of CoBLM) complexed with the self-complementary oligonucleotide d(CCAGGCCTGG) with a cleavage site at C6 has been determined by 2D NMR spectroscopic methods and molecular dynamics calculations. Intermolecular NOEs (60 between CoBLM A2 green and DNA) and intramolecular NOEs (61 within CoBLM A2 green) have defined the position and orientation of CoBLM A2 green with respect to its single binding site in the duplex. CoBLM A2 green is a stable analog of the activated BLM, the Fe^{3+} hydroperoxide (Sam, J. W.; Tang, X.-J.; Peisach, J. *J. Am. Chem. Soc.* **1994**, *116*, 5250−5256). These studies have provided the first structural insight into the mode of binding of the bithiazole tail of CoBLM A2 green to DNA, the basis for specificity of its cleavage at pyrimidines (Py) in d(G-Py) sequences, and the orientation of its terminal oxygen of the hydroperoxide relative to the 4′ carbon hydrogen bond being cleaved in the DNA. The bithiazole tail inserts 3′ to the C6 cleavage site from the minor groove. The terminal thiazolium ring is completely stacked between the bases of G14 and G15, while the penultimate thiazolium ring is only partially stacked between the bases of C6 and C7. The bithiazole tail thus binds via a partial intercalation mode and the DNA is unwound by 13° over the (G5·C16)∼(C6·G15)∼(C7·G14)∼(T8·A13) steps. No specific interactions between the bithiazole tail and the DNA have been identified, and thus, this interaction does not define the BLM's cleavage specificity but its binding affinity. The metal binding domain and the peptide linker region of CoBLM A2 green bind within the minor groove of the duplex and define the basis for its specificity of DNA cleavage. The 4-amino group and the N3 of the pyrimidine ring of CoBLM A2 green form specific hydrogen bonds with the N3 and the 2-amino group, respectively, of the G5 in the duplex and provide an unusual example of a minor groove base triple-like interaction. A basis for the preference for G over A, 5′ to the Py cleavage site, is thus established. The metal binding domain and the valeryl moiety in the linker have a conformation strikingly similar to that defined in the free CoBLM A2 green (Wu, W.; Vanderwall, D. E.; Lui, S. M.; Tang, X.-J.; Turner, C. J.; Kozarich, J. W.; Stubbe, J. *J. Am. Chem. Soc.* **1996**, *118*, 1268−1280). The most remarkable feature of this structure is the observation of the proton associated with the hydroperoxide of CoBLM A2 green and its observed intermolecular NOEs to the minor groove protons of C6 and C7 of the duplex. Thus this structure provides a rare snapshot of an analog of a reactive intermediate poised to initiate the hydrogen atom abstraction event. The molecular modeling reveals that the distal oxygen of the hydroperoxide is 2.5 Å from the 4′-hydrogen of C6. A number of additional intramolecular hydrogen bonds between the hydroperoxide ligand and the peptide linker region are also proposed, which appear to play a key role in positioning the reactive intermediate near the hydrogen atom being abstracted. This structural model makes a number of predictions that can be tested experimentally given the recent modular synthesis of BLM (Boger, D. L.; Teramoto, S.; Honda, T.; Zhou, J. *J. Am. Chem. Soc.* **1995**, *117*, 7338−7343).

Introduction

The bleomycins (BLMs) are a family of glycopeptide antibiotics used clinically in the treatment of head and neck and testicular cancers.[1] Their mode of cytotoxicity has been proposed to be related to their ability to bind to and cleave DNA.[2,3] Despite the intensive investigation of the BLMs in the last two decades, however, the basis for the specificity of BLM for cleavage at pyrimidines in d(G-Py) sequences and the mode of its binding to DNA have remained controversial and elusive. While most investigators agree that the positively charged bithiazole tail of BLM (Figure 1) provides the binding affinity of the drug for DNA,[2,3] it is less clear whether that is its sole role or whether it is important, as is the metal binding domain,[2,3] for defining the sequence selectivity.

Given these ambiguities, we decided to investigate the structural details of the interaction of BLM with DNA using 2D NMR and X-ray crystallographic methods. Other investigators have used a similar approach as evidenced by the recent

† Departments of Chemistry and Biology, Massachusetts Institute of Technology.

‡ University of Maryland.

§ Francis Bitter Magnet Laboratory, Massachusetts Institute of Technology.

|| Both authors contributed equally to this work.

⊥ Present address: Merck Research Laboratories, P.O. Box 2000, Rahway, NJ 07065-0900.

* Authors to whom correspondence should be addressed.

⊗ Abstract published in *Advance ACS Abstracts,* January 15, 1996.

(1) (a) Sikic, B. I., Rozencweig, M., Carter, S. K., Eds. In *Bleomycin Chemotherapy*; Academic Press: Orlando, FL, 1985. (b) Umezawa, H. In *Anticancer agents based on natural product models*; Cassady, J. M., Douros, J., Eds.; Academic Press, Inc.: New York, 1980; Vol. 16, pp 147−166. (c) Hecht, S. M. Ed. In *Bleomycin: Chemical, Biochemical, and Biological Aspects*; Springer-Verlag: New York, 1979.

(2) Stubbe, J.; Kozarich, J. W. *Chem. Rev.* **1987**, *87*, 1107−1136.

(3) Kane, S. A.; Hecht, S. M. In *Progress in Nucleic Acid Research and Molecular Biology*; Cohn, W. E., Moldave, K., Eds.; Academic Press: San Diego, CA, 1994; Vol. 49, pp 313−352.

0002-7863/96/1518-1281$12.00/0

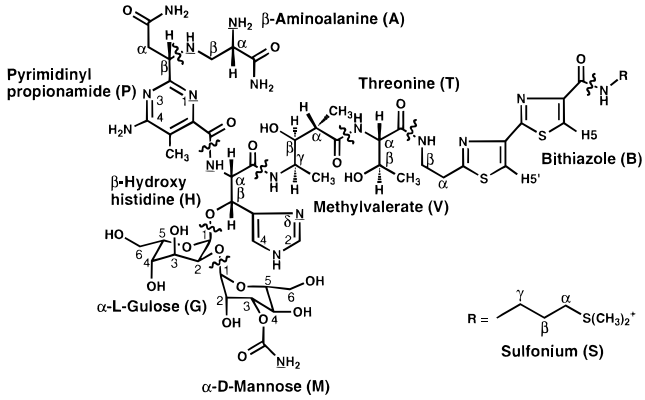

Figure 1. Structure of bleomycin A2.

and past literature on the determination of the structure of a variety of metallo-BLMs including ZnBLM,[4] FeBLM-CO,[5] and CoBLMs.[6,7] In addition, several investigators have also reported efforts to look at metallo-BLMs with oligonucleotide duplexes.[8−10] All of these studies have been unsuccessful in elucidation of the two predominant structural questions: (1) What is the mode(s) of binding of the bithiazole tail, and (2) what defines the specificity of the cleavage event?

We have chosen to examine the interaction of CoBLM A2 green with decameric oligonucleotides. Moreover, the CoBLM A2 green, as delineated in the accompanying paper,[7] was chosen for a number of reasons. First, the specificity of CoBLM A2 green mediated DNA degradation is very similar to that of the FeBLM.[11] The CoBLM A2 green is diamagnetic, and the cleavage of DNA requires light[12] and is not affected by the presence of O_2.[11] Thus, the problems associated with paramagnetism of FeBLM and its O_2-mediated cleavage are avoided with the cobalt congener. Second, as described in the preceding paper,[7] we have been able to purify and structurally characterize the hydroperoxide form of the CoBLM A2 (designated CoBLM A2 green or CoOOH). It is remarkably stable at neutral pH, and the ligands are exchange inert. Third, this CoOOH is an excellent analog of the FeOOH, that is, the activated BLM.[13] Fourth, CoBLMs were demonstrated by Chang and Meares to bind to generic DNA ($K_d \sim 10^{-7}$ M) 10-fold more tightly than the FeBLM.[11] As reported previously, we have shown that CoBLM A2 green can bind to the self-complementary d(CCAGGCCTGG) (**1**) with an apparent K_d of 1.6×10^{-7} M and that, in the presence of light, this duplex is cleaved selectively at C6.[7] Fifth, early studies of Xu et al.[14] alluded to the possibility that CoBLMs bound to DNA would be in slow exchange on the NMR time scale, which has been shown to be the case with **1**.[15]

We now report the details of our efforts using 2D NMR methods and molecular modeling to successfully determine the solution structure of CoBLM A2 green−DNA complex and elucidate the mode of binding of the bithiazole tail of CoBLM A2 green and the basis for its sequence specificity. These results also shed insight on how a single molecule of BLM can effect double-stranded, blunt-ended cleavage in duplex DNA and make a number of predictions that can be tested experimentally given the recent modular synthesis of BLM analogs.[16]

Materials and Methods

Sample Preparation. The decamer d(CCAGGCCTGG) was synthesized on a 10 μmol scale at the MIT biopolymer lab and characterized as described in the accompanying paper.[7] The purified DNA was desalted in a dialysis chamber against 50 mM sodium phosphate, pH 6.8. CoBLM A2 green was prepared using a modified published procedure.[7,17]

NMR Experiments. All NMR experiments were performed on 750 or 500 MHz Varian NMR spectrometers or on 600 or 500 MHz home-built instruments at the Francis Bitter Magnet Laboratory. Data were then transferred to a Silicon Graphics work station and processed using Felix software (version 2.3, Biosym Technologies, Inc.). ^{1}H and ^{13}C chemical shifts are referenced to an internal standard, sodium 3-(trimethylsilyl)-1-propanesulfonate at 0.00 ppm. ^{31}P chemical shifts are referenced to an external sample of trimethyl phosphate, which is 3.53 ppm downfield of 85% H_3PO_4.

A typical NMR sample contained ~3 mM complex and 50 mM sodium phosphate at pH 6.8 and was prepared by adding sequential amounts of CoBLM A2 green to the DNA sample until a 1:1 complex was apparent by NMR spectroscopy. For experiments in D_2O, the complex sample was lyophilized three times from 99.9% D_2O and then dissolved in 99.996% D_2O; for the experiments in H_2O, the complex was dissolved in 90% H_2O/10% D_2O.

DQF-COSY, TOCSY (MLEV-17 spin lock pulse with 35, 70, and 100 ms mixing times), and NOESY (50, 200, and 400 ms mixing times) experiments were recorded at 20 °C in D_2O or H_2O. Selected experiments were also recorded at 10 and 30 °C. Data sets with 4096 × 512 complex points were acquired with sweep widths of 5500 Hz (500 MHz instrument) or 8000 Hz (750 MHz instrument) in both dimensions and 32 scans per t_1 increment. During the relaxation delay period, a 2.0 s presaturation pulse was used for solvent suppression. For the NOESY experiments in H_2O, a jump and return pulse sequence[18] was used and data sets with 4096 × 512 complex points were acquired with sweep widths of 12 000 Hz in both dimensions. The t_1 dimension was zero-filled to 4096 data points, and spectra were processed with a combination of exponential and Gaussian weighting functions or a phase-shifted sine-bell weighting function. In all cases, ridges in t_1 were reduced by multiplying the first point in t_1 by one-half prior to the Fourier transform. Baselines are corrected with a polynomial or an automatic baseline correction routine in t_2 when necessary.

HMQC[19] spectra were recorded at 20 °C in D_2O with a J_{C-H} coupling constant of 135, 165, or 195 Hz. Data sets with 2048 × 256 complex points were acquired with 6000 Hz (^{1}H) and 25 000 Hz (^{13}C) sweep widths on a 500 MHz instrument. A total of 128 scans were collected for every t_1 increment. During the relaxation delay period, a 1.5 s presaturation pulse was used for solvent suppression. The t_1 dimension was zero-filled to 2048 data points. Spectra were then process with an exponential weighting function.

(4) Akkerman, M. A. J.; Haasnoot, C. A. G.; Hilbers, C. W. *Eur. J. Biochem.* **1988**, *173*, 211−225.
(5) Akkerman, M. A. J.; Neijman, E. W. J. F.; Wijmenga, S. S.; Hilbers, C. W.; Bermel, W. *J. Am. Chem. Soc.* **1990**, *112*, 7462−7474.
(6) Xu, R. X.; Nettesheim, D.; Otvos, J. D.; Petering, D. H. *Biochemistry* **1994**, *33*, 907−916.
(7) Wu, W.; Vanderwall, D. E.; Lui, S. M.; Tang, X.-J.; Turner, C. J.; Kozarich, J. W.; Stubbe, J. *J. Am. Chem. Soc.* **1996**, 118, 1268−1280 (preceding paper in this issue).
(8) Gamcsik, M. P.; Glickson, J. D.; Zon, G. *J. Biomol. Struct. Dyn.* **1990**, *7*, 1117−1133.
(9) Hiroaki, H.; Nakayama, T.; Ikehara, M.; Uesugi, S. *Chem. Pharm. Bull.* **1991**, *39*, 2780−2786.
(10) (a) Manderville, R. A.; Ellena, J. F.; Hecht, S. M. *J. Am. Chem. Soc.* **1994**, *116*, 10851−10852. (b) Manderville, R. A.; Ellena, J. F.; Hecht, S. M. *J. Am. Chem. Soc.* **1995**, *117*, 7891−7903.
(11) Chang, C.-H.; Meares, C. F. *Biochemistry* **1984**, *23*, 2268−2274.
(12) Chang, C.-H.; Meares, C. F. *Biochemistry* **1982**, *21*, 6332−6334.
(13) Burger, R. M.; Peisach, J.; Horwitz, S. B. *J. Biol. Chem.* **1981**, *256*, 11636−11644.
(14) Xu, R. X.; Antholine, W. E.; Petering, D. H. *J. Biol. Chem.* **1992**, *267*, 950−955.
(15) Wu, W.; Vanderwall, D. E.; Stubbe, J.; Kozarich, J. W.; Turner, C. J. *J. Am. Chem. Soc.* **1994**, *116*, 10843−10844.
(16) (a) Boger, D. L.; Colletti, S. L.; Honda, T.; Menezes, R. F. *J. Am. Chem. Soc.* **1994**, *116*, 5607−5618. (b) Boger, D. L.; Honda, T.; Dand, Q. *J. Am. Chem. Soc.* **1994**, *116*, 5619−5630. (c) Boger, D. L.; Honda, T.; Menezes, R. F.; Colletti, S. L. *J. Am. Chem. Soc.* **1994**, *116*, 5631−5646. (d) Boger, D. L.; Honda, T. *J. Am. Chem. Soc.* **1994**, *116*, 5647−5656.
(17) Chang, C.-H.; Dallas, J. L.; Meares, C. F. *Biochem. Biophys. Res. Commun.* **1983**, *110*, 959−966.
(18) Guéron, M.; Plateau, P.; Decorps, M. *Prog. Nucl. Magn. Reson. Spectrosc.* **1991**, *23*, 161.
(19) Bax, A.; Subramanian, S. *J. Magn. Reson.* **1986**, *67*, 565−569.

A 2D indirect detection $^{31}P-^{1}H$ COSY experiment[20] in D_2O was recorded at 20 and 30 °C on a 600 MHz instrument. Data sets with 4096 × 128 complex points were acquired with 7000 Hz in the ^{1}H dimension and 2000 Hz in the ^{31}P dimension. Data processing was carried out as described before.

Molecular Modeling. All calculations were carried out with Quanta 4.0/CHARMm 22 (Molecular simulations, Inc.; Waltham, MA) on a Silicon Graphics 4D/35 or Indigo. Nonbonded van der Waals and electrostatic interactions were cut off at 11.5 Å, using a cubic switching function between 9.5 and 10.5 Å. The distance-dependent dielectric constant algorithm in the CHARMm package was used. Hydrogen bonds were cut off at 5.0 Å and switched between 3.5 and 4.5 Å. Hydrogen bonds were also cut off at 90° and switched between 50° and 70°. Nonbonded and hydrogen bond terms were updated every 20 steps. The SHAKE algorithm[21] was used to fix all bond lengths to hydrogen atoms. Molecular dynamics calculations used the Verlet algorithm, with a 0.001 ps time step and scaling every 100 steps. During molecular dynamics all force constants for bond distances and angles were set at 1000 kcal mol^{-1} $Å^{-2}$ and 500 kcal mol^{-1} rad^{-2}, respectively. All energy minimizations used the standard CHARMm potential.[22] Distance constraints were applied using a square well potential, and dihedral constraints were applied using a simple harmonic function.

Bleomycin A2 was constructed in Chemnote as described in detail in the preceding paper.[7] The DNA was constructed in Quanta assuming a B-form conformation. Since no counterions or solvent molecules were used in these studies, the charges on the nonbridging oxygens of the phosphate groups were reduced to lower the overall charge on phosphate to −0.32.[23] Color figures were made using Setor.[24] DNA conformational parameters were measured using NEWHELIX93 (Protein Data Bank).

Experimental Constraints. Intramolecular NOEs within DNA or within CoBLM A2 green and intermolecular NOEs between the DNA and CoBLM A2 green were classified as strong, medium, or weak on the basis of visual inspection of the cross peak intensities in the 200 ms NOESY spectra. CoBLM−DNA intermolecular and CoBLM A2 green intramolecular NOE-derived distance constraints were set at 1.9−3.0, 1.9−4.0, and 3.0−5.0 Å for strong, medium, and weak NOEs, respectively. An additional 1 Å was added to the upper limit of constraints on methyl or methylene hydrogen pseudoatoms. DNA intramolecular constraints were set at 1.9−3.0, 2.5−4.0, and 3.5−5.0 Å for strong, medium, and weak NOEs, respectively.

For CoBLM A2 green itself,[7] the generalized Karplus equation that considers the electronegativity of substituents was used to derive the dihedral angle constraints.[25] In the 1D or 2D spectra of the CoBLM A2 green complexed with DNA, spectral broadening (line width > 5 Hz) and overlap have placed constraints on accurate assessment of the coupling constants. The analysis of the coupling constants in CoBLM A2 green is thus based on visual inspection of the cross peak sizes in the DQF-COSY spectrum. A large coupling constant (>10 Hz) has been used to define a trans orientation of the protons involved, while a small coupling constant (<5 Hz) has been used to define a gauche conformation.

For DNA, the backbone angles, α, β, γ, ϵ, and ζ, were constrained to B-form values,[26] with force constants applied as described in the molecular dynamics section. The δ and χ angles were not constrained. Dihedral angle constraints with a force constant of 30 kcal mol^{-1} $Å^{-2}$ rad^{-2} were used throughout the molecular dynamics simulations on the DNA base pairs to prevent excessive propeller twist and buckling. These constraints were not applied at the intercalation site (C6·G15 and C7·G14).

Initial Structure. The initial structure was constructed by manually docking the bithiazole moiety between C6·G15 and C7·G14. Only one orientation of the bithiazole with respect to the DNA, and of each of the thiazolium rings with respect to one another was consistent with the observed NOEs. This was confirmed in the preliminary modeling in which the bithiazole moiety alone was placed >7 Å from DNA, and the molecular dynamics with the intermolecular NOE constraints consistently resulted in the same orientation of the bithiazole moiety between C6·G15 and C7·G14. The bithiazole, threonine, and valeryl (B, T, V, Figure 1) backbone dihedral angles were manipulated to relieve bad contacts between the metal binding region and the minor groove. After this crude positioning, the structure was minimized by 200 steps of the steepest descent method, followed by conjugate gradient minimization to a rms gradient of <0.1. The structure was then further minimized by the conjugate gradient method using the dihedral and distance constraints, to a rms gradient of <0.1.

Molecular Dynamics. To begin the restrained molecular dynamics simulated annealing, the distance constraints on the initial structures used a force constant of 0.6 kcal mol^{-1} $Å^{-2}$. The structure was heated and equilibrated over 4 ps, from 5 to 1000 K in 10 K increments, with velocities assigned every 0.1 ps from a Gaussian approximation to the Maxwell−Boltzman distribution. The force constants for the distance constraints were then scaled to 120 kcal mol^{-1} $Å^{-2}$ over 6.5 ps. The system was allowed to evolve for 10 ps, then cooled to 300 K over 7 ps. At 300 K the force constants of the distance constraints were reduced to the final value of 60 kcal mol^{-1} $Å^{-2}$. The dihedral constraints were then introduced with a force constant of 5 kcal mol^{-1} rad^{-2} and increased to 50 kcal mol^{-1} rad^{-2} in four stages over 10 ps. The dihedral angle constraints on the DNA backbone angles β, γ, and ϵ at the intercalation site and the adjacent base pairs were applied with force constants of 5 and 10 kcal mol^{-1} rad^{-2}, respectively. The electrostatic and hydrogen bond energy terms were introduced, and the system was allowed to equilibrate for 4 ps, followed by a final 30 ps molecular dynamics run. The system was coupled to a heat bath at 300 K with a time factor of 0.1 ps during the final 30 ps.

The structures from the final 5 ps of the 30 ps molecular dynamics simulations were averaged and minimized. One-thousand steps of conjugate gradient minimization with the distance constraints and CoBLM dihedral angle constraints were used. The DNA backbone constraints were not used in the minimization. This process was repeated from a starting structure using eight different seeds for initial velocity assignments.

Results and Discussion

In preliminary experiments we reported that titration of d(CCAGGCCTGG) (**1**) with CoBLM A2 green resulted in the formation of a 1:1 complex that is in slow exchange on the NMR time scale.[15] The 1D ^{1}H NMR spectrum of the titration in the range of 0.5−3.0 ppm is shown in supporting Figure 1. The free oligonucleotide **1** is self-complementary and hence gives rise to one set of resonances for symmetry-related protons (e.g., T-CH_3 at 1.68 ppm). Titration with CoBLM A2 green resulted in new sets of resonances corresponding to the CoBLM−DNA complex in which the symmetry has been disrupted (T8-CH_3 (1.64 ppm) and T18-CH_3 (1.72 ppm), supporting Figure 1).

In addition, upon binding of CoBLM A2 green to the oligonucleotide, the chemical shift of the methyl group of the pyrimidine moiety of the drug in the metal binding region (Figure 1) has changed from 2.48 to 2.61 ppm and the two equivalent terminal methyl groups (2.94 ppm) of the sulfonium moiety (Figure 1) have become nonequivalent (2.97 and 3.00 ppm) (supporting Figure 1). In contrast, the peak intensities and chemical shifts of the α and γ methyl groups of the methylvaleryl moiety (V) and the methyl group of the threonine moiety (T), both in the peptide linker region of CoBLM A2 green, are almost identical to those in the free CoBLM (Table 1 and supporting Figure 1). These resonances thus conveniently provided the starting points for the assignments of V and T spin systems.

(20) Maudsley, A. A.; Ernst, R. R. *Chem. Phys. Lett.* **1977**, *50*, 368−372.
(21) van Gunsteren, W. F.; Berendsen, H. J. C. *Mol. Phys.* **1977**, *34*, 1311−1327.
(22) Brooks, B. R.; Bruccoleri, R. E.; Olafson, B. D.; States, D. J.; Swaminathan, S.; Karplus, M. *J. Comput. Chem.* **1983**, *4*, 187−217.
(23) Manning, G. S. *Q. Rev. Biophys.* **1978**, *II*, 179−246.
(24) Evans, S. V. *J. Mol. Graphics* **1993**, *11*, 134−138.
(25) Haasnoot, C. A. G.; De Leeuw, F. A. A. M.; Altona, C. *Tetrahedron* **1980**, *36*, 2783−2792.
(26) Dickerson, R. E. *Methods Enzymol.* **1992**, *211*, 67−111.

Table 1. Proton and Carbon Chemical Shifts (ppm) of Free CoBLM A2 Green and CoBLM A2 Green Complexed with DNA

		carbons		protons				carbons		protons	
		free, pH 6.8, 5 °C	complex, pH 6.8, 20 °C	free, pH 6.8, 5 °C	complex, pH 6.8, 20 °C			free, pH 6.8, 5 °C	complex, pH 6.8, 20 °C	free, pH 6.8, 5 °C	complex, pH 6.8, 20 °C
P	CαH	35.5		3.20	2.78	B	CαH′	35.5	34.7	3.25	2.76
	CαH′	35.5		3.51	3.69		CβH	41.9		3.44	2.93
	CβH	65.1	65.7	5.10	5.16		CβH′	41.9		3.83	3.76
	CH_3	12.0	12.3	2.46	2.61		C5H	127.5	126.8	8.17	7.26
	4-NH_2			7.73,7.94	7.14,10.36		C5′H	121.3	117.5	7.82	7.21
H	CαH	60.1	62.0	4.98	5.01		NH			8.57	8.62
	CβH	71.7	73.3	5.53	5.48	S	CαH_2	43.4	43.4	3.36	3.56, 3.46
	C2H	144.8	146.5	8.72	9.10		CβH_2	26.6	25.7	2.13	2.07, 2.16
	C4H	122.2	122.0	7.60	7.60		CγH	40.3	40.0	3.51	3.43
A	CαH	59.3	60.0	3.41	3.37		CγH′	40.3	40.0	3.63	3.43
	CβH	51.8	50.3	2.74	2.46		$(CH_3)_2$	27.3	27.4	2.94	2.97, 3.00
	CβH′	51.8	50.3	3.22	3.24		NH			8.66	7.81
	NH			6.01	5.69	G	C1H	97.4	99.9	5.35	5.40
V	αCH_3	9.8	9.6	0.62	0.65		C2H	69.9		4.11	4.04
	γCH_3	20.4	20.4	0.98	0.96		C3H	68.4		4.10	4.13
	CαH	42.9	42.8	0.94	1.21		C4H	71.8		3.80	3.73
	CβH	77.7	76.1	3.33	3.73		C5H	70.8		3.84	
	CγH	49.6	50.4	3.50	3.51		C6H	63.9		3.70	
	NH			8.89	8.78		C6H′	63.9		3.84	
	OH				6.79	M	C1H	98.5	103.3	4.93	4.95
T	CH_3	22.4	21.6	1.19	1.23		C2H	70.3		4.00	3.96
	CαH	60.0	59.6	4.39	4.53		C3H	77.6		4.05	
	CβH	71.7		4.25	4.51		C4H	66.7		3.78	
	NH			8.92	9.36		C5H	77.0		3.73	
B	CαH	35.5	34.7	3.06	2.83		C6H	63.5		3.84	
							C6H′	63.5		3.98	
						CoOOH					8.89

Table 2. Proton and Phosphorus Chemical Shifts (ppm) of DNA in the Complex at 20 °C

	H6/ H8	H5/ H2	methyl	H1′	H2′	H2″	H3′	H4′	H5′,5″	^{31}P		H6/ H8	H5/ H2	methyl	H1′	H2′	H2″	H3′	H4′	H5′,5″	^{31}P
C1	7.77	5.96		5.95	2.12	2.53	4.69	4.12	3.77	−0.66	C11	7.74	5.94		5.94	1.99	2.45	4.65	4.11	3.73	−0.61
C2	7.58	5.70		5.49	2.14	2.49	4.88	4.13		−0.44	C12	7.58	5.70		5.13	2.12	2.29	4.79	4.05		−0.28
A3	8.35	7.50		5.96	2.85	2.85	5.07	4.41	4.15, 4.06	−0.78	A13	8.00	7.89		5.99	2.53	2.72	5.01	4.33	4.07, 3.91	−0.82
G4	7.56			5.87	2.40	2.82	5.03	4.42	4.14	−0.96	G14	7.38			5.23	2.42	2.72	5.02	4.31	4.10	1.71
G5	7.81			5.41	2.68	2.36	4.97	4.45	4.21	0.91	G15	7.60			5.73	2.52	2.71	4.79	4.44	4.29, 4.00	−1.18
C6	7.43	5.59		5.98	1.76	2.36	4.81	3.25	3.81, 4.00	−0.84	C16	7.36	5.25		5.52	2.30	2.30	4.77	4.26	4.13	−0.44
C7	7.63	5.97		5.91	2.21	2.25	4.77	3.98	3.74, 3.32	−0.82	C17	7.59	5.53		5.98	1.94	2.64	4.79	3.60	3.95	−0.83
T8	7.34		1.64	5.53	2.09	2.26	4.82	4.14	4.05, 3.95	−0.30	T18	7.14		1.72	5.44	1.70	2.02	4.71	3.73	3.93, 3.89	−0.52
G9	7.85			5.69	2.73	2.73	4.99	4.36	3.98, 4.08	−0.44	G19	7.81			5.71	2.68	2.72	4.98	4.37	4.06, 3.94	−0.55
G10	7.84			6.12	2.56	2.33	4.67	4.19	4.19, 4.11		G20	7.77			6.11	2.51	2.33	4.64	4.19		

	imino	C amino		imino	C amino		imino	C amino
C1·G20			G5·C16	12.91	8.55, 6.35	G9·C12	13.15	8.56, 6.96
C2·G19	12.91	8.65, 6.95	C6·G15	12.54	7.79, 6.59	G10·C11		
A3·T18	14.62		C7·G14	11.84	8.23, 7.18			
G4·C17	13.24	8.96, 6.81	T8·A13	14.24				

Proton and Carbon Assignments of the CoBLM A2 Green in the Complex. For the V spin system, proton assignments were established through the expected connectivity patterns in the DQF-COSY and TOCSY spectra in H_2O and D_2O. The cross peak between V-CαH and V-CβH, however, is absent in the COSY and TOCSY spectra, indicating a small coupling constant between these two protons. This observation along with the unusual upfield chemical shift of the V-αCH_3 (0.65 ppm) is also apparent in the free CoBLM A2 green (Table 1). Nevertheless, a strong NOE between the V-CαH and the V-CβH as well as NOEs to other protons within the spin system confirms the assignments. Additional confirmation comes from the carbon chemical shifts for this spin system, which have been assigned using the HMQC method. The carbon chemical shifts of the V-αCH_3, V-γCH_3, V-αC, V-βC, and V-γC are very similar to those in the free CoBLM (Table 1). When a COSY spectrum was run in H_2O, an exchangeable proton at 6.79 ppm was observed which showed a cross peak to the V-CβH proton. This proton also showed TOCSY cross peaks to V-CβH and V-CγH and NOEs to all the methylvaleryl protons (Table 3). This resonance was thus assigned to the proton of the β-OH group of V, suggesting that it must be H-bonded in the complex with DNA. This proton, as expected, is not detected in the free CoBLM A2 green.

The proton chemical shift assignments for the T, the β-hydroxyhistidine (H), and the pyrimidinylpropionamide (P) spin systems (Figure 1) were obtained by inspection of the COSY and TOCSY spectra in both H_2O and D_2O (Table 1). The identification of the T-CH_3 resonance (1.23 ppm) facilitated the assignment of T-CαH and T-CβH. The T-NH is shifted 0.44 ppm downfield relative to its chemical shift in the free CoBLM A2 green and showed a TOCSY cross peak to the T-CαH in H_2O. Similarly, through-bond connectivities are observed from H-CαH to H-CβH, H-C2H to H-C4H (weak four-bond coupling), and P-CαHs to P-CβH. Intramolecular NOEs between protons in these spin systems are all consistent with these

Table 3. Nontrivial Intramolecular NOEs within CoBLM A2 Green in the Complex at 20 °C[a]

H-C2H- - -A-CβH	w	G-C1H- - -H-CαH	m	B-NH- - -B-CαH′	m
H-C2H- - -A-CβH′	w	A-CβH- - -P-CαH′	m	V-NH- - -V-CαH	s
H-C2H- - -A-NH	m	A-CβH′- - -P-CαH′	w	S-CαH- - -S-CH_3(1)	w
H-C2H- - -P-CβH	w	A-CβH- - -P-CβH	w	S-CαH′- - -S CH_3(1) and (2)	w
H-C2H- - -T-CH_3	m	A-CβH′- - -P-CβH	w	V-OH- - -V-CαH	w
H-C2H- - -T-CβH	w	A-CβH′- - -P-CαH	m	V-OH- - -V-αCH_3	w
H-C2H- - -T-CαH	w	A-CαH- - -P-CαH	w	V-OH- - -V-γCH_3	s
H-C2H- - -T-NH	w	A-CβH- - -P-CαH	m	V-OH- - -V-CβH	s
H-C2H- - -V-CαH	m	V-γCH_3- - -P-CH_3	w	P-NH_2(1)- - -P-CH_3	m
H-C2H- - -V-αCH_3	w	V-αCH_3- - -V-CγH	s	P-NH_2(2)- - -P-CH_3	m
H-C2H- - -V-CβH	w	V-γCH_3- - -V-CβH	s	CoOOH- - -V-NH	w
H-C4H- - -V-CαH	w	V-αCH_3- - -V-CβH	m	CoOOH- - -T-NH	m
H-C4H- - -V-αCH_3	m	V-αCH_3- - -V-γCH_3	m	CoOOH- - -V-αCH_3	w
H-C4H- - -H-CαH	w	V-γCH_3- - -V-CαH	m	CoOOH- - -V-γCH_3	w
A-NH- - -T-CH_3	w	T-NH- - -V-CαH	m	CoOOH- - -V-CγH	w
P-CβH- - -B-CβH	w	T-NH- - -V-NH	m	CoOOH- - -V-CαH	m
G-C1H- - -H-CβH	s	V-NH- - -V-γCH_3	s	CoOOH- - -P-CβH	m
G-C1H- - -M-C1H	m	V-NH- - -V-αCH_3	s	CoOOH- - -V-OH	w
V-CγH- - -H-CβH	w	B-NH- - -T-CαH	m	CoOOH- - -A-NH	w
V-αCH_3- - -H-CβH	w	B-NH- - -T-CH_3	m	CoOOH- - -H-C2H	w
M-C1H- - -H-CβH	w	B-NH- - -B-CαH	m		

[a] w, m, s: weak, medium, strong NOE at 200 ms mixing time. P-NH_2(1), 10.36 ppm; P-NH_2(2), 7.14 ppm. S-CH_3(1), 3.00 ppm; S-CH_3(2), 2.98 ppm.

assignments. In none of the experiments recorded in H_2O was the amide proton of the β-hydroxyhistidine (H-NH) observed. This result is consistent with previous studies on other metallo-BLMs in which there is general agreement that this amide is deprotonated and is one of the ligands to cobalt.[4,5]

The assignment of the protons associated with the bithiazole moiety (Figure 1) of CoBLM A2 green is essential to defining its mode of binding to the DNA duplex. As previously reported by Akkerman et al., the H5 proton of the terminal thiazolium ring and the H5′ of the penultimate thiazolium ring can be assigned using HMQC and HMBC methods.[5] We have used these methods to unambiguously assign B-C/H5 (127.5 and 8.17 ppm) and B-C/H 5′ (121.3 and 7.82 ppm) in the free CoBLM A2 green. The HMBC method applied to the complex has been unsuccessful because of the signal-to-noise and overlap problems. However, we have previously reported use of the HMQC method to assign the two bithiazole protons to resonances at 7.21 and 7.26 ppm. By making the assumption that the ^{13}C chemical shift of the carbon attached to each of these protons in the complex has not dramatically shifted relative to those in the free CoBLM A2 green, the resonance at 7.21 ppm has been assigned to the B-H5′ (B-C5′ at 117.5 ppm) and the one at 7.26 ppm to B-H5 (B-C5 at 126.8 ppm).

The identification of the methylene protons associated with the bithiazole moiety of CoBLM A2 green has proven more difficult due to the spectral overlap with the H2′ and H2″ protons of DNA in the region 2−3 ppm. Initially, the B-CαHs and B-CβHs were located using a TOCSY experiment in H_2O in which cross peaks have been detected between the B-NH proton and these two sets of protons. Subsequent re-examination of the COSY and TOCSY spectra collected in D_2O confirm the assignments via the through-bond couplings between B-CαHs and B-CβHs. Further confirmation of these assignments is provided by the observation of strong intramolecular NOEs between the B-NH proton and the T protons and trivial NOEs within the B spin system itself.

For the assignments of the proton chemical shifts in the dimethylsulfonium (S) spin system (Figure 1), the methylene protons of CαH, CβH, and CγH show strong COSY cross peaks to each other and to their adjacent protons. In the TOCSY spectrum collected in H_2O, the amide proton (S-NH) is easily identified through its cross peak to S-CγH at a short mixing time (35 ms) and to both S-CγH and S-CβH at a longer mixing time (70 ms). The assignments of the S spin system and bithiazole ring protons are corroborated by a weak NOE between B-C5H and S-CγH in the NOESY spectrum at 400 ms mixing time (absent at 200 ms mixing time). The carbon chemical shifts of the sulfonium group, assigned using the HMQC method, exhibit little variation with respect to the free CoBLM A2 green (Table 1).

The most difficult chemical shift assignments have been associated with the β-aminoalanine moiety (A), the axial ligand of CoBLM A2 green. In the TOCSY or the COSY spectra in H_2O, the secondary amine (A-NH) has not been located. Furthermore, in the DQF-COSY and TOCSY experiments collected in D_2O, no ABX spin system could be assigned to the A-CαH proton and the A-CβH protons. The chemical shift assignments of this spin system have been achieved as outlined subsequently. Protons with chemical shifts at 2.46 and 3.24 ppm are strongly coupled to each other in the DQF-COSY spectrum, and both show weak NOEs to the P-CβH proton (Table 3). These protons were initially assigned to the A-CβHs. A resonance at 3.37 ppm was assigned to the CαH on the basis of its strong NOEs to both A-CβHs and a weak NOE to the P-CαH. As further confirmation of these tentative assignments, the carbon chemical shifts of the A-αC and A-βC in the free CoBLM A2 green at 59.3 and 51.8 ppm, respectively, were compared with the ^{13}C chemical shifts associated with the putative A-Cα and A-Cβ in the complex: 60.0 and 50.3 ppm. These similarities support the above assignments. Finally, re-examination of the NOESY spectrum in H_2O allowed us to assign the A-NH proton (5.69 ppm), which shows trivial NOEs to A-CβHs as well as several additional, structurally informative, intramolecular NOEs (Table 3).

The absence of the COSY cross peaks between the A-CαH and A-CβHs is attributed to the small coupling constants between these protons, which is reminiscent of the small values (3 and 4 Hz) observed between the same set of protons in the free CoBLM A2 green. On the basis of the arguments presented in the preceding paper,[7] the small coupling constants between the A-CαHs and A-CβHs in the complex are consistent with the model in which the primary amine of A serves as an axial ligand to cobalt. Thus, the identity of this axial ligand in CoBLM A2 green is similar to that in its complex with DNA.

The final assignments in CoBLM A2 green to be made are the protons associated with the gulose (G) and mannose (M) residues. Unfortunately, these protons reside in a region of the spectrum (∼4 ppm) which has extensive overlap with the 4′

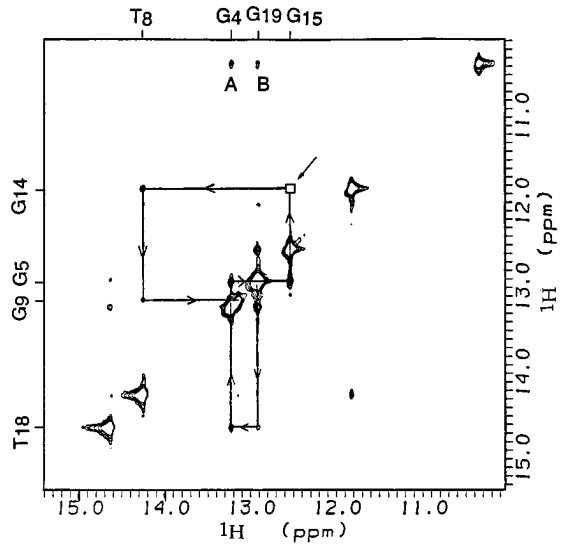

Figure 2. Imino to imino region of the NOESY spectrum (200 ms mixing time, 500 MHz) of a 1:1 complex of CoBLM and **1** in H_2O. CoBLM A2 green and **1** (5.0 mM) in 90% H_2O/10% D_2O in 50 mM sodium phosphate (pH 6.8) at 20 °C. The sequential imino to imino cross peaks are traced by connecting lines. The missing NOE between the imino proton of G14 to that of G15 is indicated by a box. Intermolecular NOEs are (A) P-NH_2 (10.36 ppm) to the imino proton of G4·C17 and (B) P-NH_2 (10.36 ppm) to the imino proton of G5·C16.

and 5′ protons of the deoxyribose of the DNA. Despite this spectral crowding, DQF-COSY and TOCSY spectra have allowed assignments of G-H1′ through G-H4′ for gulose and M-H1′ and M-H2′ for mannose (Table 1).

Assignment of the Exchangeable Protons of the DNA in the Complex. A 1D ^{1}H NMR spectrum of the complex in H_2O at 20 °C displays eight imino resonances, whereas in the free DNA, only four imino protons are observed. At 5 °C, all five imino protons of the free DNA are observed with the terminal G·C imino hydrogen, as expected, being very broad. These results, described previously by Wu et al.,[15] indicate that the formation of a 1:1 complex of the DNA with CoBLM A2 green results in the disruption of the DNA symmetry.

The assignments of the imino protons have been made using standard NOESY experiments. The two most downfield resonances are at 14.62 and 14.24 ppm and have been assigned to the two thymine imino protons of T18 and T8, respectively, on the basis of their strong NOEs to their base-pairing adenine H2. The assignments of the adenine H2, in D_2O, are confirmed by the observed weak NOEs (400 ms mixing time) to their own H1′, the 3′-neighboring H1′, and the 5′-neighboring H1′ on the opposite strand.

Sequential imino−imino NOEs from the two A·T imino protons have allowed assignment of all the remaining imino protons with the exception of terminal G·C base pairs and those associated with C6·G15 and C7·G14. As outlined below the connectivity between the base pairs associated with C6 and C7 is disrupted due to the intercalation between them of the bithiazole ring tail of CoBLM A2 green (Figure 2). The imino protons of the terminal G·C pairs are not observed at 20 °C, presumably due to exchange broadening. The guanine imino protons also show strong NOEs to the protons of the 4-amino groups and weak NOEs to the H5 protons of their base-paired cytosine partners. Each cytosine amino proton also exhibits strong NOEs to its own H5 proton.

Two exchangeable protons with unusual chemical shifts have also been detected whose assignments have provided much structural insight. The proton at 8.89 ppm is proposed to be associated with CoBLM A2 green, and the other proton at 10.36 ppm, tentatively assigned to the G5 amino proton of the DNA,[15] is, as outlined below, also shown to be associated with CoBLM A2 green. It is one of the protons of the 4-amino group attached to the pyrimidine ring (Figure 1). The reassignment of the proton at 10.36 ppm is based on its strong NOE to another exchangeable proton at 7.14 ppm, the second proton of the amino group of the pyrimidine ring, and the fact that both 4-amino protons show medium NOEs to the P-CH_3 (Figure 1). Additional NOEs to the DNA (for example to G5-H4′, Table 4) and molecular modeling described subsequently support this assignment. The interaction of a G5 amino proton with its G5-H4′ would have required a drastic distortion of the generic B-form DNA as the distance between these protons is greater than 7 Å in B-form DNA. No evidence for this type of distortion exists from a detailed analysis of the sugar puckers of the deoxyribose rings outlined below. Second, there is no detectable NOE between the amino proton at 7.14 ppm and the G5·C16 imino proton as would be expected if this proton were associated with the amino of G5. Thus the unusual downfield shifted amino proton of P from 7.94 or 7.73 ppm in the free CoBLM A2 green to 10.36 ppm in the complex and its NOEs to DNA have important structural implications.

The second exchangeable proton of interest at 8.89 ppm has

Table 4. Intermolecular NOEs between CoBLM A2 Green and DNA at 20 °C

5′ end	strand 1	BLM residues	3′ end	strand 2	BLM residues
A3			T18	H4′	P-CαH/w
				H4′	A-CαH/m
				H5′* [b]	A-CαH/s
G4	NH	P-NH_2(1)[a]/w	C17	H1′	A-CαH/w
				H4′	A-CβH′/w
					A-CβH/w
					A-CαH/s
					P-CαH/w
G5	H4′	P-CH_3/m	C16		
		P-NH_2(1)/w			
		P-NH_2(2)/w			
	H1′	P-CH_3/w			
		P-NH_2(1)/m			
		P-NH_2(2)/m			
	NH	P-NH_2(1)/w			
C6	H5″	P-CH_3/s	G15	H1′	B-C5H/w
		V-$\gamma$$CH_3$/m		H4′	B-C5H/w
	H5′	P-CH_3/s		H5′	B-C5H/m
		V-$\gamma$$CH_3$/m		NH	B-C5H′/m
	H4′	CoOOH/m			B-CβH′/w
		P-CH_3/m			B-CβH/w
		V-$\gamma$$CH_3$/m		H8	B-C5H/m
	H2″	CoOOH/w			
	H2′	CoOOH/w			
	H1′	CoOOH/m			
		P-CH_3/w			
		P-CβH/m			
	NH2h	B-C5H′/m			
	NH2e	B-C5H′/m			
C7	H5″	T-CαH/m	G14	H1′	B-C5H/s
	H5′	CoOOH/w		H2″	B-C5H/s
		V-OH/w		H2′	B-C5H/m
		T-CαH/m		H3′	B-C5H/w
	H4′	CoOOH/w		H4′	B-C5H/w
		T-CH3/w		NH	B-C5H′/w
		T-CαH/m		H8	B-C5H/m
		B-NH/m			S-CβH′/w
	H1′	B-CαH′/w			S-CβH/w
		B-CαH/w			S-CγH/m
		B-NH/m			
T8			A13	H8	S-CH_3/w
3′ end	strand 1		5′ end	strand 2	

[a] P-NH_2(1) and P-NH_2(2) are the hydrogens at 10.36 and 7.14 ppm, respectively. [b] Used the H5′ pseudoatom.

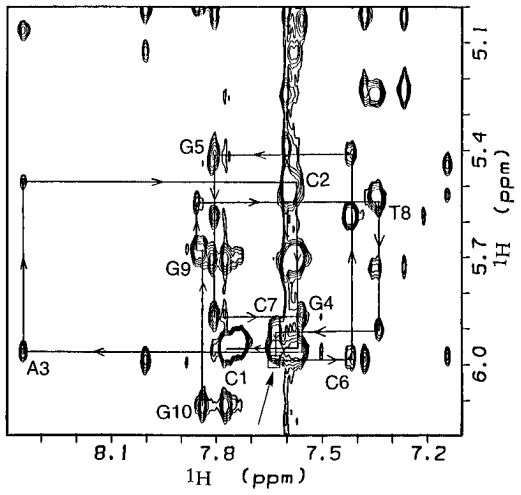

Figure 3. Expanded NOESY spectrum (400 ms mixing time, 500 MHz) of the base to sugar H1′ region of strand 1 (C1∼C2∼A3∼G4∼G5∼C6∼C7∼T8∼G9∼G10) in the complex. The sequential connectivities are indicated by the connecting lines, and the break in the sequential connectivities at the C6∼C7 step is shown by an arrow with a box.

been assigned to the proton associated with the axial hydroperoxide ligand of CoBLM A2 green. This resonance shows six NOEs to the C6 and C7 sugar protons of DNA (Table 4) and 10 NOEs to the protons associated with the metal binding region and the V and T moieties in the peptide linker of CoBLM A2 green (Table 3). A number of additional facts allow us to favor this unusual assignment. No scalar connections from this proton to other protons can be observed in either the TOCSY or the COSY spectra. No NOEs are detected between this proton and any of the imino or amino protons associated with the DNA, thus making it unlikely that it is a proton associated with the decamer itself. Finally, the possibility that this proton is associated with one of the unassigned exchangeable protons of CoBLM A2 green, such as the primary amine of the A or terminal amino protons of the primary amides, can be ruled out because NOE patterns expected from these amino protons are incompatible with the NOE patterns associated with this resonance.[27] As outlined below, molecular modeling provides very strong support for this unusual and structurally significant assignment.

Assignment of the Nonexchangeable Protons of DNA in the Complex. Protons associated with DNA bases and sugars have been assigned by analyzing the NOESY, TOCSY, DQF-COSY, and ^{31}P−^{1}H COSY spectra using standard sequential strategies.[28] The assignments are summarized in Table 2, and the sequential connectivities for strands 1 and 2 of the decamer are summarized in Figure 3 and Figure 2 (supporting information).

For strand **1** (C1 to G10), the sequential base to base and base to H1′ NOEs can be readily traced from the H8 of G10 to the H6 of C7. There are no NOEs observed, however, from the H6 of C7 to the H6 of C6 or from the H6 of C7 to the H1′ of C6 (Figure 3). The disruption of this connectivity revealed in the final structural model is a function of the penultimate thiazolium ring being stacked between C6 and C7. By starting with C6, one can easily follow the sequential connectivity from C6 to the C1 (Figure 3). For strand **2** (C11 to G20, supporting Figure 2), the sequential NOEs can be followed from G20 to G15. No connectivity is observed between the H8 of the G15 and the H8 of the G14 due to the intercalation of the terminal thiazolium ring between these two bases. However, in the region between 7.6 and 5.9 ppm, there is extensive spectral crowding and therefore, it is not possible to assess if the connectivity from the G15-H8 to G14-H1′ has been interrupted as would be predicted from the final model. The sequential NOEs from G14 to C11 are readily observed (supporting Figure 5).

The sugar protons (H2′, H2″, H3′, and H4′) of each nucleotide have been assigned by their connectivities with their own H1′ protons using TOCSY experiments carried out at various mixing times (30 ms for H2′ and H2″; 70 and 100 ms for H3′ and H4′). The H2′ protons have been distinguished from the H2″ protons using the NOESY spectrum collected at 50 ms mixing time, where regardless of the sugar pucker the NOE between the H1′ and the H2″ should be larger than that between the H1′ and the H2′.[29] In the DQF-COSY spectrum, all H1′ to H2′ cross peaks, except for C6, are indicative of sugars having C2′-endo-like puckers. For C6 (the site of CoBLM A2 green light mediated cleavage), the H1′ to H2″ and H3′ to H4′ cross peaks are readily detected, while the H1′ to H2′ is absent. These observations are consistent with a C3′-endo-like sugar pucker.[29] The implications of the altered sugar pucker of C6 will be discussed subsequently.

The assignments for H2′ and H2″ have been confirmed using a NOESY experiment (200 ms) by tracing the NOEs between the base to its own 2′ and 2″ protons and the sequential NOEs between the base and its 5′-neighboring H2′ and H2″. No NOEs are observed between the H6 of the C7 to H2′ and H2″ of C6. The NOEs between the H8 of G15 to the H2′ and H2″ of the G14 are obscured due to spectral crowding. The H3′ proton assignments can also be confirmed using the 200 ms NOESY experiment by following the sequential NOEs between the base to its own and to its 5′-neighboring H3′ protons.

The assignments for the H5′ and H5″ of the DNA are more problematic due to spectral crowding. TOCSY experiments using long mixing times (100−200 ms) have not allowed the assignments of H5′ and H5″ from H1′. Attempts to use the DQF-COSY method to identify cross peaks between H4′ to H5′ and H5″ were also unsuccessful because of spectral crowding between 4 and 4.5 ppm (Table 2). Thus assignments of the H5′ and H5″ protons were made in the ^{31}P−^{1}H spectrum (vide infra), as well as in the NOESY spectrum by assuming a standard B-form DNA structure, where weak NOEs from the base proton to its own H5′ and H5″ would be expected to be observed. As noted in Table 2, some of these assignments were still not possible.

Assignments of the Carbons of DNA in the Complex. The HMQC spectrum has been useful since the carbon chemical shifts associated with the bases and the deoxyribose residues are predictable, that is, they are not altered substantially between the free and the complexed DNA. Thus association of a carbon with a proton having an unusual chemical shift would provide further confirmatory evidence for the proton assignment. Two examples of the usefulness of the data from an HMQC spectrum follow. First, the chemical shift of the H4′ of C6 has been assigned to 3.24 ppm, dramatically upfield shifted in comparison with the other H4′ protons (Table 2). The HMQC spectrum reveals a carbon chemical shift of 83.8 ppm associated with

(27) Recent studies with CoBLM A2 brown (in which an H_2O ligand has replaced the hydroperoxide ligand) demonstrate that it binds **1** in an analogous fashion to CoBLM A2 green. The exchangeable proton, however, at 8.89 ppm is absent.

(28) Wüthrich, K. *NMR of Proteins and Nucleic Acids*; John Wiley & Sons, Inc: New York, 1986.

(29) (a) Majumdar, A.; Hosur, R. V. *Prog. NMR Spectrosc.* **1992**, *24*, 109. (b) Hosur, R. V.; Ravikumar, M.; Chary, K. V. R.; Sheth, A.; Govil, G.; Zu-Kum, T.; Miles, H. T. *FEBS* **1986**, *205*, 71−76. (c) van Wijk, J.; Huckriede, B. D.; Ippel, J. H.; Altona, C. *Methods Enzymol.* **1992**, *211*, 286−306.

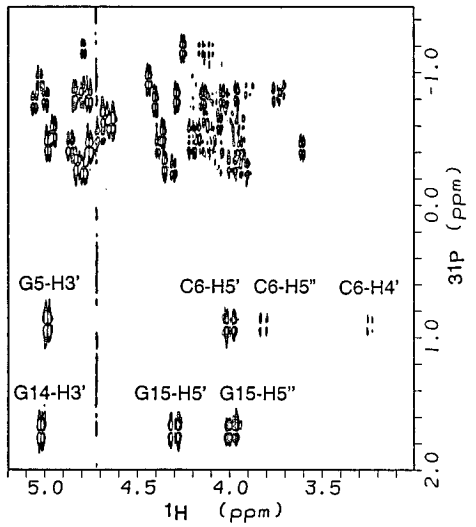

Figure 4. $^{31}P-^{1}H$ COSY spectrum of the complex at 30 °C.

this proton. This chemical shift is typical of C4′ carbons,[30] and thus, this method provides additional confidence in the proton assignment. A second interesting example is provided by C7-H5″ which has been upfield shifted dramatically relative to other H5′/H5″ protons to 3.32 ppm. The carbon chemical shift associated with this proton is 66.7 ppm, typical of a C5′ of a deoxyribose moiety.[30] These protons with unusual chemical shifts have been highlighted as they possess interesting intermolecular NOEs to CoBLM A2 green (Table 4). The correct assignments of these shifted protons have been essential in the structure elucidation.

^{31}P Assignments of DNA in the Complex. In the free DNA, nine DNA phosphorus resonances are present, which become doubled in the presence of CoBLM A2 green. Two of the phosphorus signals are downfield shifted from the normal envelope of the ^{31}P resonances and have been assigned to the phosphates connecting G5∼C6 and G14∼G15 using a $^{31}P-^{1}H$ COSY spectrum (Figure 4). This type of downfield movement is indicative of an intercalative mode of binding for CoBLM A2 green.[31]

Finally, the $^{31}P-^{1}H$ COSY experiment also provides an independent verification of the assignments of the H3′ and some of the H4′ and H5′/H5″ protons of the deoxyribose residues. Eighteen phosphorus to H3′ cross peaks are discernible and assigned by the correlation between the ^{31}P and its 5′-coupled H3′. Additionally, ^{31}P is coupled to its 3′-neighboring H4′ and H5′/H5″. Although the complete sequential assignments from the phosphorus to the H4′, H5′/H5″ protons have not been attainable because of overlap, the assignments of sugar protons near the intercalation site are confirmed (Figure 4).

Molecular Modeling

Distance Constraints. Intramolecular NOEs within DNA or within CoBLM A2 green and intermolecular NOEs between DNA and CoBLM A2 green were classified on the basis of visual inspection of the cross peak intensities in the 200 ms NOESY spectra collected in H_2O and D_2O. There are total of 60 intermolecular NOEs (Table 4), 61 intramolecular CoBLM NOEs (Table 3), 206 intramolecular DNA NOEs, and 28 Watson−Crick hydrogen bond constraints.

Dihedral Constraints. Ten dihedral angle constraints of CoBLM A2 green were derived as described in Materials and Methods. DNA backbone β, γ, and ϵ angles have been constrained using standard B-form DNA parameters.[26] Lower force constants were used on the base pairs of the intercalation site, and those directly adjacent to it, to allow for potential distortion of the DNA as a result of the intercalation of the bithiazole moiety. The use of generic DNA constraints was based on a qualitative analysis of the NMR data, which suggested, with the exception of the structural variations described below, that the DNA backbone was not significantly distorted. It was found that, in the preliminary structural calculations, these constraints significantly improved the fit of the structure to the NOE data. Additionally, no notable NOE violations were observed in the region of DNA in contact with CoBLM A2 green, thus the reduced force constants of the dihedral angle constraints in this region allowed sufficient flexibility to satisfy the experimental data. The constraints for the backbone α and ζ angles were qualitatively derived from the ^{31}P chemical shift information (Table 2) in the complex[32] as discussed subsequently. In duplex B-form DNA, the gauche(−), gauche(−) (g^-,g^-; ζ,α) geometry about the P−O bonds in the backbone is energetically favored, and this geometry is associated with a more shielded ^{31}P resonance. The other significantly populated conformation, the trans, gauche(−) (t,g^-; ζ,α) geometry, results in a more downfield shifted ^{31}P resonance.[32] Accordingly, the two downfield shifted phosphates (Figure 4) in our complex, one between G5 and C6 and the other between G14 and G15, were constrained to the trans and gauche(−) conformation for the ζ and α angles, respectively, while the remaining phosphates have been constrained to the gauche(−) and gauche(−) geometries for these angles, respectively.

The range of pseudorotation angles for each sugar pucker has been estimated from the analysis of the consecutive intranucleotide sugar proton coupling constants in the DQF-COSY spectrum in D_2O.[29] In particular, the size of the coupling constants of H1′−H2′, H2″−H3′, and H3′−H4′ are informative because of their sensitivity to the sugar conformation. In a generic C2′-endo sugar pucker, a large coupling constant for H1′−H2′ is expected, while both the coupling constants for H2″−H3′ and H3′−H4′ are small. For a generic C3′-endo sugar pucker, a small coupling constant is expected for H1′−H2′, while large coupling constants are expected for H2″−H3′ and H3′−H4′. In the eight calculated structures, the pseudorotation angles were found to be consistent with experimentally determined ranges. In particular, the pseudorotation angle of the cleavage site C6 was 70° ± 5°, consistent with a C3′-endo-like sugar pucker as previously mentioned.

The glycosidic torsion angles, χs, were determined from the intensity of the intranucleotide H8/H6-H1′ NOEs.[33] Nucleotides with a *syn* glycosidic conformation have a characteristic short distance of ∼2 Å that will be observed in NOESY spectrum at a short mixing time. In the complex of CoBLM A2 green with DNA, no intranucleotide H8/H6-H1′ NOEs were observed above the background in the NOESY spectrum at 50 ms mixing time. Thus, all the nucleotides in the complex were expected to be in *anti* conformations with χ angles between −72° and −180° and all the structures were found to lie within this range.

Molecular Dynamics Studies. A structure for the complex of CoBLM A2 green with DNA was obtained using NOE distance constraints derived from NMR experiments and molecular modeling methods as outlined subsequently. The initial

(30) Leupin, W.; Wagner, G.; Denny, W. A.; Wüthrich, K. *Nucleic Acids Res.* **1987**, *15*, 267−275.

(31) (a) Gao, X.; Patel, D. J. *Biochemistry* **1988**, *27*, 1744−1751. (b) Addess, K. J.; Gilbert, D. E.; Olsen, R. K.; Feigon, J. *Biochemistry* **1992**, *31*, 339−350.

(32) Gorenstein, D. G. *Methods Enzymol.* **1992**, *211*, 254−286.

(33) Kim, S.; Lin, L.; Reid, B. R. *Biochemistry* **1992**, *31*, 3564−3574.

Table 5. Structural Statistics

total number of distance constraints	352
CoBLM−DNA intermolecular	60
CoBLM intramolecular	61
DNA intramolecular	203
DNA base pair H-bond	28
rms deviation from experimental distance constraints in the eight calculated structures (Å)	0.034 ± 0.002
maximum error (Å)	0.174 ± 0.015
Σ distance constraint errors (Å)	4.723 ± 0.288
rms deviation from dihedral angle constraints in the eight calculated structures (deg)	5.18 ± 0.92
rms deviation from experimental distance contraints in the minimized average structure (Å)	0.037
maximum error	0.200
Σ distance constraint errors (Å)	5.134
rms deviation from dihedral angle constraints in the minimized average structure (deg)	4.50
pairwise rms deviation among the eight calculated structures (Å)	
all atoms	1.248
all atoms, excluding DNA ends, and CoBLM S, G, and M moieties[a]	0.615
CoBLM, excluding S, G, and M	0.502
pairwise rms deviation of the eight calculated structures relative to the minimized average structure (Å)	
all atoms	1.375
all atoms, excluding DNA ends, and CoBLM S, G, and M moieties	0.706
CoBLM, excluding S, G, and M	0.653

[a] DNA nucleotides 3−8, and 13−18, and the bound CoBLM A2 green without the sugars (G and M) or the sulfonium tail (S).

starting structure was constructed by positioning the bithiazole moiety of the previously determined solution structure of CoBLM A2 green (structure I, Figure 7a of the preceding paper[7]) between the C6·G15 and C7·G14 base pairs. The initial orientation was based on the NOE data described above showing specific interactions of B-H5 and B-H5′ with residues of G14, G15, and C6 (Table 4). This initial structure was then submitted to minimizations and molecular dynamics simulated annealing calculations described in the Materials and Methods. An overlay of the structures from the eight separate calculations are shown in Figure 3 (supporting information). A summary of results from the structural calculations is presented in Table 5. The final distances are in very good agreement with rms deviations from the distance constraints of 0.034 ± 0.002, and no constraint errors are over 0.2 Å. A final structure was obtained by averaging eight separately determined structures, followed by the minimization of the averaged coordinates. This structure is the basis for the remaining discussion.

Overall Structure. The minimized structure is shown in Figure 5. The model reveals, as indicated by preliminary studies of Wu et al.,[15] that the bithiazole tail binds via partial intercalation between base pairs C6·G15 and C7·G14 with the sulfonium tail extending into the major groove. This intercalation site is 3′ to the cleavage site at C6. The metal binding region is positioned within the minor groove with a number of contacts between the drug molecule and the DNA (Table 4). Specific contacts between G5 and the pyrimidine moiety of the drug suggest a basis for sequence specificity. This structure also positions the distal oxygen of the metal-bound peroxide, approximately 2.5 Å from the 4′-hydrogen of C6, the site of C−H bond cleavage. The model as presented provides insight into the mode of binding of CoBLM A2 green to DNA, the molecular basis for the observed specificity, and the mechanism of cleavage of DNA. In the following sections each of these unique features of the structure in Figure 5 will be presented and discussed.

Binding. Multiple modes of binding for metallo-BLMs have been suggested since its discovery.[2,3] Some investigators have focused on potential minor groove binding properties of the B moiety based on its similarity in structure relative to other known minor groove binders such as distamycin and netropsin.[34] The sequence specificity has been suggested to be related to the 2-amino group of guanine 5′ to the cleavage site, which provides a hydrogen bond to the nitrogen(s) of the thiazolium rings of the B moiety.[35] Recent NMR studies by Hecht and co-workers with ZnBLM have been interpreted to indicate that one mode of binding to a defined oligonucleotide is within the minor groove.[10] Their studies are complicated, however, by the observation of multiple binding motifs and minimal NOEs.[10] In addition, the relationship between ZnBLM and the Fe or CoBLMs is not clear because ZnBLM is structurally unique[36] among metallo-BLMs and is chemically unreactive.

Other investigators have interpreted their physical and biochemical studies to support a mode of binding that involves partial intercalation of the B moiety of the drug.[8,37] Studies of Williams and Goldberg using a series of bulged oligonucleotides have suggested the BLM's mode of binding involving bithiazole intercalation, would require its insertion 3′ to the cleavage site.[38] Recent 2D NMR studies from our laboratory[15] have provided the first direct evidence for this intercalative model and are elaborated herein.

The key to defining the mode of binding of B has been identification of the B-H5 and B-H5′ protons using heteronuclear NMR methods presented in the accompanying paper.[7] These protons are upfield shifted 0.91 and 0.61 ppm, respectively, from the chemical shifts observed with the free CoBLM A2 green, a hallmark of intercalation.[39a] Complete assignments of the protons of CoBLM A2 green in the complex (>85%) and of the DNA protons (>95%) has allowed us to identify the interactions of these B protons with the DNA (Tables 3 and 4). These NOEs define the position of the B within the base-pairing

(34) (a) Dickerson, R. E. In *Mechanism of DNA Damage and Repair: Implications for Carcinogenesis and Risk Assessment Basic Life Sciences*; Smi, M. G., Grossman, L., Eds.; Plenum: New York, 1986; Vol. 38, pp 245−255. (b) Klevit, R. E.; Wemmer, D. E.; Reid, B. R. *Biochemistry* **1986**, *25*, 3296.

(35) Kuwahara, J.; Sugiura, Y. *Proc. Natl. Acad. Sci. U.S.A.* **1988**, *85*, 2459−2463.

(36) On the basis of the arguments presented in the preceding paper[7] and as shown in the studies of Akkerman et al. on ZnBLM,[4] for the Zn to accommodate both the primary amine of A and the carbamoyl nitrogen of M as axial ligands, it must adopt a structure similar to III in the preceding paper[7] (Figure 7c).

(37) Povirk, L. F.; Hogan, M.; Dattagupta, N. *Biochemistry* **1979**, *18*, 96−101.

(38) Williams, L. D.; Goldberg, I. H. *Biochemistry* **1988**, *27*, 3004−3011.

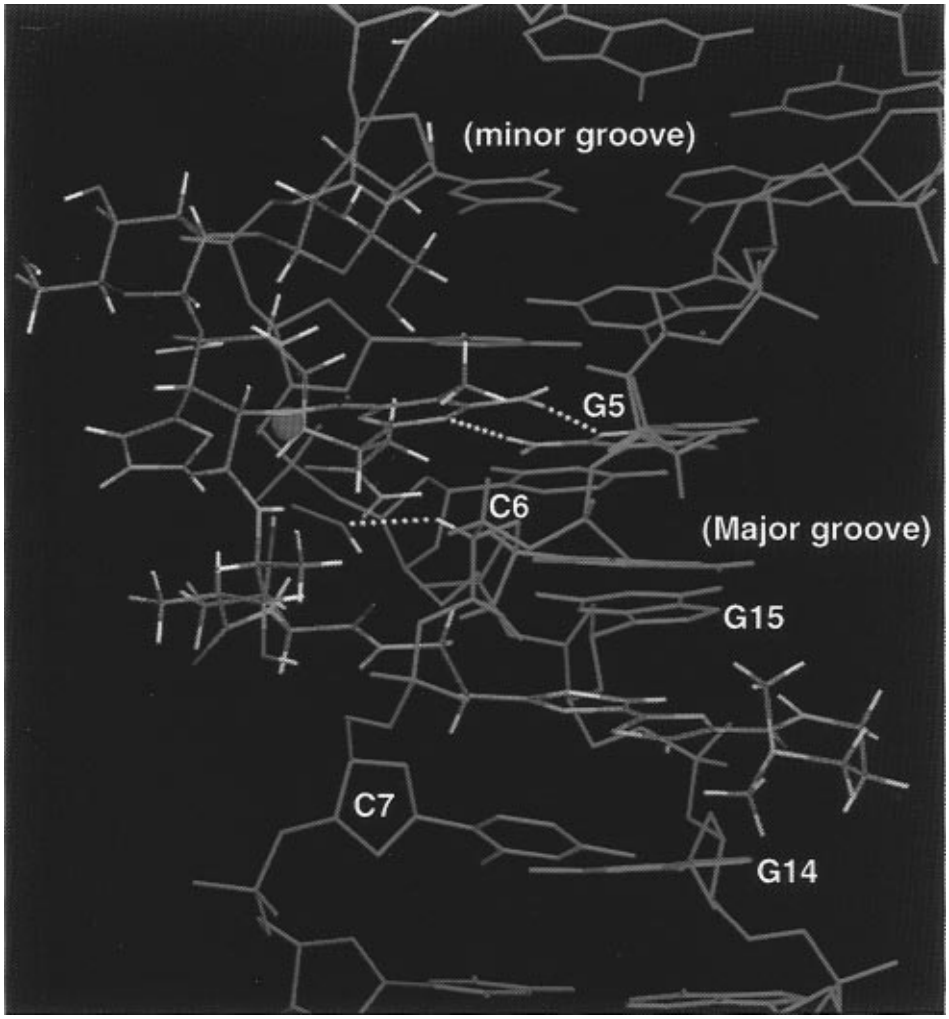

Figure 5. Structure of Co·BLM A2 green (atoms colored by element: C = green, O = red, N = blue, and S = yellow) bound to DNA (purple, C6-H4′ = white). The damaged strand is in the foreground, running 5′ → 3′ from the upper right to lower left corner. The dotted lines indicate the H-bond interactions between the P moiety of CoBLM and the G5 of the DNA. Also indicated is the proximity of the distal oxygen of the hydroperoxide ligand to the C6-H4′ (2.5 Å).

structure and also define the orientation of the side chain extending out from the intercalation site. In addition, the NOEs between the B-CαH and B-NH and the DNA (H1′ of C7 for example in Table 4) suggest unambiguously that intercalation occurs from the minor groove 3′ to the cleavage site.

The present solution structure provides us with a model for the B moiety in the complex (Figure 6). The terminal thiazolium ring is in the trans configuration[39b] and is completely stacked between the bases of G14 and G15. The plane of the terminal thiazolium ring essentially assumes the position of another base, approximately 3.4 Å from the planes of G14 and G15 bases. This model is supported by the ^{31}P NMR experiments which indicate that the phosphorus between G14 and G15 is shifted downfield by ∼2 ppm. The penultimate thiazolium ring is only partially stacked between the bases of C7 and C6. This model is in agreement with previous studies of many investigators on FeBLMs (summarized in a review by Stubbe and Kozarich[2]) where the data supported a partial rather than a complete mode of intercalation. For example, DNA unwinding studies reveal an unwinding of 12° by FeBLM rather than 23° for a classic parallel intercalator such as ethidium bromide.[40]

In the present structure, the DNA is distorted in a manner more consistent with a "perpendicular" rather than "parallel" intercalator.[41] The DNA is unwound a total of ∼13° over the three steps, (G5·C16)∼(C6·G15)∼(C7·G14)∼(T8·A13). The intercalation site is only unwound ∼6°, whereas the base step after it is unwound by ∼8.5°, and the step before the intercalation site slightly overwound by ∼1.5°. The base pairs before and after the intercalation site are also buckled by −7.8° and 25.2°, respectively, a conformational feature also found in the X-ray crystal structures of daunomycin and nogalamycin.[42] This buckling has been proposed to increase favorable van der Waals contact between the drug and DNA.

The question can be raised as to whether the mode of binding for d(GpC) steps in the present studies are similar to d(GpT) steps. Results reported in the preceding paper with an oligonucleotide containing a d(GTAC) ds-cleavage site suggest a

(39) (a) Although the penultimate thiazolium ring as a whole is partially stacked between the bases of C6 and C7, the B-H5′ proton is positioned almost directly below the base of C6, which causes the upfield chemical shift change (0.61 ppm) due to the ring current effect. The B-H5 proton is completely stacked between G14 and G15 (Figure 9) and thus experiences even larger upfield chemical shift change (0.91 ppm). (b) The bithiazole tail is sufficiently flexible in the free CoBLM A2 green such that the orientation of the thiazolium rings relative to one another is not discernible.

(40) (a) Tsai, C.; Jain, S. C.; Sobell, H. M. *J. Mol. Biol.* **1977**, *114*, 301−305. (b) Tsai, C.; Jain, S. C.; Sobell, H. M. *J. Mol. Biol.* **1977**, *114*, 317−331.

(41) Williams, L. D.; Egli, M.; Gao, Q.; Rich, A. *DNA Intercalation: Helix Unwinding and Neighbor-Exclusion*; Adenine Press: Schenectady, NY, 1992.

(42) (a) Frederick, C. A.; Williams, L. D.; Ughetto, G.; van der Marel, G. A.; van Boom, J. H.; Rich, A.; Wang, A. H. *Biochemistry* **1990**, *29*, 2538−2549. (b) Gao, Y.; Liaw, Y.; Robinson, H.; Wang, A. H. *Biochemistry* **1990**, *29*, 10307−10316.

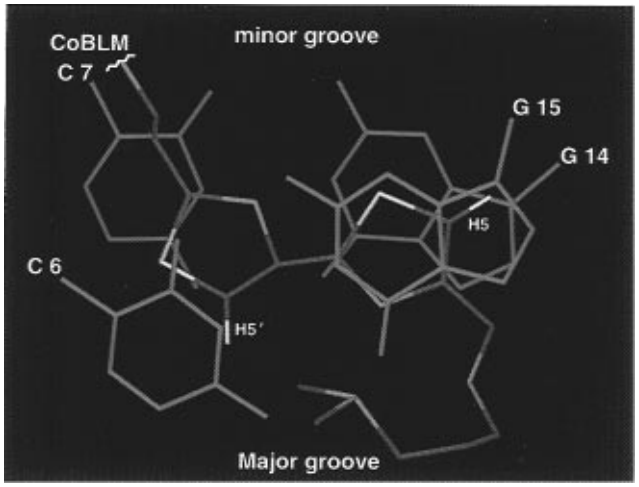

Figure 6. Binding by partial intercalation of the bithiazole tail of CoBLM A2 green to DNA. A view looking down the helical axis showing the terminal thiazolium ring stacked between the bases of G14 and G15 and the penultimate thiazolium ring partially stacked between the bases of C6 and C7. Also shown is the kinked sulfonium tail close to the major groove as evidenced by the NOE between one of the sulfonium methyls and A13-H8.

partial intercalative mode of binding at this site as well.[7] In fact, many of the features reported with **1** are also apparent with a second oligomer, d(CCAGTACTGG).

The model in Figure 6 also suggests a role for the sulfonium ion in the intercalation phenomenon. The nonequivalence of the sulfonium ion methyl groups (supporting Figure 1) and a key observed NOE between one methyl group of S and A13-H8 reflects the limited range of motion of the sulfonium ion tail within the major groove. This observation requires that the intercalation of the B moiety extends into the major groove. The positioning of the sulfonium ion suggests a role for this group in anchoring the intercalated bithiazole, through an electrostatic interaction between the positively charged sulfonium group and the negatively charged region of the major groove. This would suggest that caution must be exercised in interpretation of mechanistic studies with synthetic BLM analogs lacking this group.[43,44]

The absence of any observable sequence specific interactions between the bithiazole moiety and the DNA suggests that this binding mode is not specifically inherent to any sequence motif. This is in accord with many previous studies but provides the first structural evidence in support of this hypothesis.

Specificity. The most significant prediction of our model is its clear demonstration that the basis for sequence specificity resides predominately in the metal binding domain. Many previous biochemical studies have demonstrated the importance of the 2-amino group of G in d(G-Py) sequences, for the specificity of BLM-mediated cleavage.[35,45] Our studies now provide the first molecular basis for understanding the role of the 2-amino group in specificity. In addition, these studies reveal for the first time the importance of the N3 of guanine (or any purine) in the recognition of the metallo-BLM.

The key interactions are shown in Figure 7. This structure reveals two critical H bonds between the pyrimidine of the metal binding domain of CoBLM A2 green and the G5 of the DNA sequence. The N3 of the pyrimidine on CoBLM A2 green is H-bonded to the non-base-pairing hydrogen of the 2-amino of

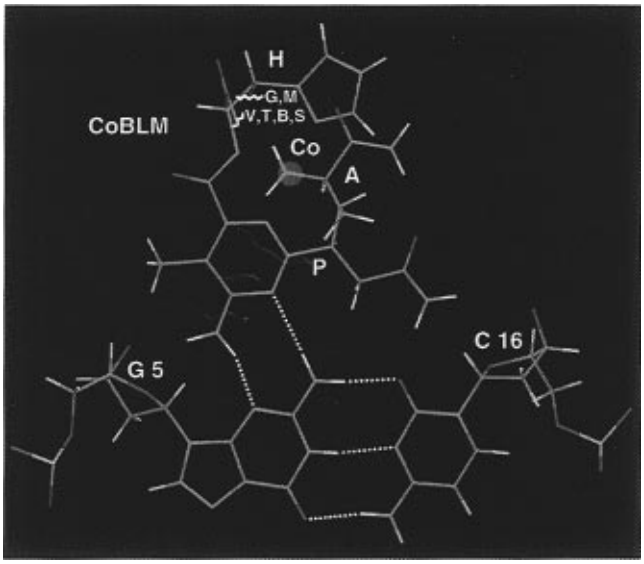

Figure 7. Basis for specificity of BLM cleavage at d(G-Py) sequences. The P moiety of CoBLM A2 green forms a minor groove base-triple-like interaction with the G5·C16 base pair. The dotted lines indicate H-bonds between the P moiety of CoBLM and G5, as well as the Watson−Crick H-bonds.

G5 of DNA at a distance[46] of 2.3 Å and an angle[46] of 176°. Second, one of the hydrogens of the 4-amino group of the pyrimidine on CoBLM A2 green is H-bonded to the N3 of G5 of DNA at a distance of 1.9 Å and an angle of 155°. The H-bonding between one of the hydrogens of the P-NH_2 group and the N3 of G5 is dramatically demonstrated in the NMR spectrum by its position at 10.36 ppm relative to that observed in CoBLM A2 green itself at 7.34 or 7.91 ppm. It is important to emphasize that this H-bonding network (Figure 7) was not used as a constraint in the molecular dynamics calculations. In fact, this H-bonding network was a result of the many intermolecular NOEs observed between the P and A moieties of the CoBLM A2 green with the DNA (Table 4). These two hydrogen bonds represent a unique base-triple-like interaction between the G5·C16 and the pyrimidine of the drug in the minor groove.

Finally, three other potential hydrogen bonds are observed in the final structure of the complex that are more speculative in nature. One is between the other the 4-amino proton of the pyrimidine on CoBLM A2 green and the O4′ of the deoxyribose ring of G5 at a distance of 2.2 Å and an angle of 143°. However, the O4′ oxygen resides in a less than ideal orientation to participate as a hydrogen bond acceptor, and thus far, there is no indication of a sugar pucker of G5 different from that expected for a generic B-form DNA that is more favorable for this H bonding interaction. The other potential hydrogen bond observed in the model is between the primary amide proton of the propionamide on CoBLM A2 green and the O2 of the C16 base (paired with G5) at a distance of 1.8 Å and an angle of 162° (Figure 7). Finally, a third putative interaction involves the carbonyl oxygen of the amide of P which is within H-bonding distance of the hydroxyl proton of the T in the linker (distance = 1.7 Å, angle = 147°). As will be discussed subsequently, the T moiety appears to participate in a number of additional putative H-bonding interactions perhaps playing a key role in the alignment of the activated oxygen species for 4′ hydrogen atom abstraction.

The interaction with N3 of the purine has not been previously suggested and may provide an explanation of the decreased

(43) (a) Carter, B. J.; Murty, V. S.; Reddy, K. S.; Wang, S.-N.; Hecht, S. M. *J. Biol. Chem.* **1990**, *265*, 4193−4196. (b) Carter, B. J.; Reddy, K. S.; Hecht, S. M. *Tetrahedron* **1991**, *47*, 2463−2474.

(44) Levy, M. J.; Hecht, S. M. *Biochemistry* **1988**, *27*, 2647−2650.

(45) Zhang, G. Ph.D. Thesis, University of Maryland, 1993.

(46) The H bond distance is between the proton and the H bond acceptor atom in all cases. The H bond angle is determined by the donor atom, the hydrogen, and the acceptor atom.

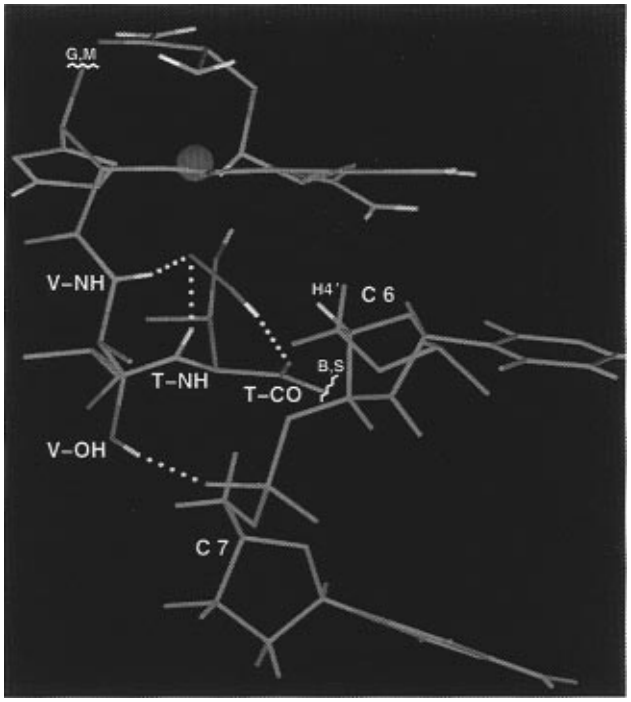

Figure 8. Position of the hydroperoxide oxygens of CoBLM A2 green relative to the 4′ hydrogen of C6, the site of cleavage. A complete hydrogen bonding network involving the hydroperoxide ligand in CoBLM A2 green complexed with DNA is apparent. H-bonds are indicated from the NH protons of V and T to the proximal hydroperoxide oxygen, the T carbonyl oxygen to the hydroperoxide hydrogen, and the V-OH to the phosphate between C6 and C7.

cleavage of pyrimidines adjacent to dAs. Although there is a loss of binding energy by the absence of the 2-amino group, one could propose that the H-bond between the NH_2 group of P and the adenine is still in place to define a weak specificity for d(A-Py). This minimal interaction would be missing at pyrimidine−pyrimidine steps.

Mascharak et al. have recently reported the synthesis of the metal binding domain of BLM missing the 4-amino group of the pyrimidine, a key H-bonding partner in our model. These analogs are reported to cleave DNA with sequence selectivity identical to that observed with metallo-BLMs.[47] In contrast, recent studies from the Hecht and Boger laboratories using a metal binding domain identical to BLM revealed no such cleavage.[3,48] Thus the basis of specificity with Mascharak's analogs is mystifying. The Hecht and Boger results clearly suggest an important interplay between the binding of the B moiety (intercalation) and the metal binding domain (selectivity) in the overall cleavage process.[3,48] In summary, our observations provide the first proposal for sequence selectivity that accounts for the specificity of G and accounts for the general observations that pyrimidines adjacent to dGs are cleaved more efficiently than pyrimidines adjacent to dAs.

Chemistry. Our structure (Figure 5) provides, to our knowledge, the first opportunity to assess a model of the reactive activated BLM (FeOOH). Furthermore, the model allows the first direct insight into the relationship between the metal and the 4′ hydrogen of the pyrimidine being cleaved. As shown in Figure 8, the calculated structure places the distal oxygen of the hydroperoxide to within 2.5 Å of the H4′ of C6, the closest DNA proton to the hydroperoxide. This interaction was not used as a constraint for calculation of the model. Instead this interaction was the result of the following set of observations. Initially the model was derived using NOE constraints from nonexchangeable protons of the metal binding domain of CoBLM A2 green with the DNA (Table 4). A key observation was that of an initially unassignable, exchangeable proton at 8.89 ppm. Subsequent to the molecular modeling, the only proton which could give rise to this exchangeable proton is that of the hydroperoxide. This result is particularly intriguing and insightful as this proton exhibits six intermolecular NOEs to C6 and C7 (Table 3), the region of DNA cleavage. While all of the exchangeable hydrogens of CoBLM A2 green and DNA have yet to be assigned, this is the only hydrogen in this region of the complex that could give rise to these NOEs. Thus, these NOE distance constraints were added to our other constraints and molecular dynamics calculations gave rise to the structure reported in Figure 8. Support for the proximity of the metal to C6-H4′ is also derived from the NMR analysis in which this hydrogen is dramatically upfield shifted from the free DNA (4.22 to 3.25 ppm).

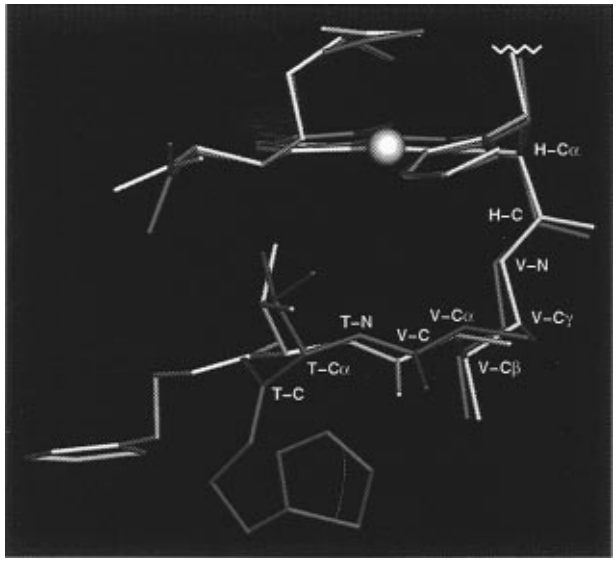

Figure 9. Overlay of CoBLM A2 green in the free (red) and the bound (white) forms, showing the high degree of similarity in the metal binding region, the V moiety, and portions of the T moiety. For clarity, only the first thiazolium ring of the B moiety is shown and the sugars are excluded.

The observation of the proton of the hydroperoxide of CoBLM A2 green is a fortuitous piece of information which allows the verification of the location of a putative reactive oxygen intermediate of the metallo-BLM relative to its site of hydrogen atom abstraction (C6-H4′). This model provides a structural basis for our previous studies which showed that metallo-BLMs cannot mediate hydrogen atom abstraction from the H1′ position of a Py. The steric and NOE constraints inherent in the model would prevent access of the hydroperoxide to this hydrogen. This model also suggests that H5′ chemistry would be difficult to effect. The distance between the distal hydroperoxide oxygen and any H5/H5″ protons is 4.2 Å or greater. Thus, for chemistry to occur at H5′/H5″ position, the movement of the metal binding region as the result of positioning the hydroperoxide ligand within a reasonable distance of the H5′/H5″ would result in the disruption of the hydrogen bonding network between the pyrimidine and the G5 of DNA.

The observation of an excellent analog of an intermediate along a reaction pathway may give a rare opportunity to

(47) Guajardo, R. J.; Hudson, S. E.; Brown, S. J.; Mascharak, P. K. *J. Am. Chem. Soc.* **1993**, *115*, 7971−7977.

(48) (a) Boger, D. L.; Teramoto, S.; Honda, T.; Zhou, J. *J. Am. Chem. Soc.* **1995**, *117*, 7338−7343. (b) Boger, D. L.; Teramoto, S.; Zhou, J. *J. Am. Chem. Soc.* **1995**, *117*, 7344−7356. (c) Boger, D. L.; Colletti, S. L.; Teramoto, S.; Ramsey, T. M.; Zhou, J. *Bioorg. Med. Chem.* **1995**, *3*, 1281−1295.

speculate on the chemistry involved in hydrogen atom abstraction of H4′ from C6. The chemistry of reactive intermediates in mononuclear non-heme systems is at present speculative based on analogy with the better characterized heme systems.[49] The question arises as to whether the hydroperoxide or an undetected additional intermediate resulting from the heterolytic or homolytic oxygen−oxygen bond cleavage of this hydroperoxide actually results in removal of the 4′ hydrogen atom. In the case of heme peroxidase systems, it is clear that appropriate acid and base catalysts are precisely positioned to assist in heterolytic oxygen−oxygen bond scission. It is speculated that heme monooxygenases involve reactive intermediates similar to heme peroxidases.

The structure in Figure 5 was therefore carefully scrutinized to identify similar groups that might assist in catalysis. No such groups are apparent. Instead the hydrogens of amide moieties of both T and V in the linker region make excellent H-bonds (1.9 and 1.8 Å), respectively, with the penultimate oxygen, not the terminal oxygen as required for a heterolytic cleavage mechanism. A third additional H-bonding interaction is also apparent between the proton of the hydroperoxide and carbonyl of the T (distance = 1.9 Å, angle = 163°). Finally, as discussed above, the hydroxyl proton of T appears to be H-bonded to the carbonyl oxygen of terminal amide of the propionamide. This H-bonding network suggests a very sequestered and ordered environment for the hydroperoxide moiety and may provide an explanation for Boger's cleavage studies using synthetic analogs modified in the linker region.[48c] They showed that the replacement of T with a glycine resulted in a FeBLM analog that cleaves DNA with 5% of the efficiency of the wild type FeBLM. Glycine is conformationally more flexible than T, and thus, the position of its carbonyl relative to the hydroperoxide could be substantially altered. Unfortunately, these observations about the hydroperoxide environment have provided no insight into the chemistry of oxygen−oxygen bond cleavage as the H-bonding network is interacting with the wrong oxygen. Instead, the H-bonding network to the penultimate oxygen may contribute to the unusual stability of the cobalt hydrogen peroxide complex (CoBLM A2 green). Given the low resolution of this structure, however, speculation about the chemistry of the hydrogen atom abstraction is thus premature.

Comparison of Free and Bound CoBLM A2 Green. The NOE patterns and the coupling constants observed for the metal binding domain and the valeryl moiety in the linker region of CoBLM A2 green in the DNA complex are similar to those observed in the free CoBLM A2 green. In particular, intramolecular NOEs from the H-C2H to the V protons are nearly identical to those reported in the previous paper, positioning the valeryl moiety underneath the metal coordination plane as observed in the free CoBLM A2 green. The absence of any observable coupling between the V-CαH and V-CβH and a large coupling constant between the V-CβH and the V-CγH essentially define the the same conformation for the V reported for free CoBLM A2 green (Figure 9).[7] The V-NH as well as T-NH is again well positioned to participate in a hydrogen-bonding network to the proximal oxygen of the hydroperoxide ligand (V-NH to O: distance = 1.8 Å, angle = 155°; T-NH to O: distance = 1.9 Å, angle = 152°).[46] An additional hydrogen bond is noted between the V-OH and one of the nonbridging oxygens of the phosphate between C6 and C7 (Figure 8), which accounts for the NMR observation of this exchangeable proton. The remainder of the T moiety and B moiety however undergoes a significant conformational reorganization as a consequence of insertion of the bithiazole rings between the base pairs (Figure 9). This is most obvious in the change of T−Cα−T−CO dihedral angle from 120° in the free CoBLM A2 green to −180° in the complex with DNA (Figure 9). This change in conformation reorients the threonine carbonyl oxygen to be in good position to act as a hydrogen-bond acceptor for the hydroperoxide hydrogen (distance = 1.9 Å, angle = 163°). The existence of such a hydrogen bond is corroborated by the observation of the exchangeable proton on the hydroperoxide.

One of the intriguing questions that can be raised is what makes the CoBLM A2 green's octahedral environment different from the octahedral environments of the previously characterized ZnBLM and FeBLM-CO. The ZnBLM, as pointed out earlier, has a dramatically altered coordination environment in that both the primary amine of A and the carbamoyl nitrogen of M are proposed to be ligands in contrast with other metallo-BLMs. This altered coordination, and hence altered structure[36] and the lack of chemical reactivity of ZnBLM, suggests that it is not a good model for metallo-BLM-mediated DNA degradation. The FeBLM-CO complex may likewise not be a good model for activated BLM, as discussed in the accompanying paper.[7] The oxidation state of iron in this complex, the absence of an appropriate "oxygen ligand", and the ability of ligands to undergo chemical exchange with other ligands all suggest that activated BLM might be structurally different from the FeBLM-CO.

New Insights and Predictions from the Structure of CoBLM A2 Green Complexed with DNA. The modular total synthesis of BLM[16] and the ability to make DNA using nucleotide analogs warrants speculative predictions from the structure reported herein. These analogs can then be examined quantitatively with regard to the binding and cleavage of defined DNA sequences and the structure determined by NMR.

The peptide linker region is of great interest in that recent studies from Boger's laboratory with mutations in this region[48] and from our own laboratories on the ds-cleavage process[50] suggest that it plays a key role in subtly coordinating binding and cleavage. Our structure suggests that one could now synthesize conformationally restrained valeryl analogs. These analogs would be predicted to accelerate rates of cleavage for FeBLM in that now all of the binding energy could be used in catalysis. The location of the V moiety in the structure provides a great deal of flexibility in synthetic design. The structure in the linker region also predicts that the T and V NHs are H-bonded to the peroxide. The importance of these H-bonds to both structure and catalysis can be assessed by the synthesis of the appropriate ester analog.

Boger's recent studies have indicated the importance of the T moiety in cleavage.[48c] In these studies however glycine replaced T. Our structure would suggest that the side chain may play a key role in defining the correct conformation of the carbonyl of the T. This model can also be tested experimentally using constrained T analogs. Quantitative differences can be assessed by examining the binding and cleavage and comparison with the structural information. The model for ds cleavage we have recently put forth suggests, as originally proposed by Povirk,[51] that a single molecule of BLM can effect cleavage on both strands of DNA without dissociation from the DNA. This model requires flexibility in the linker region, which could be readily tested quantitatively with linkers of constrained conformations and our assay for ds cleavage.[50]

(49) English, A. M.; Tsaprailis, G. *Adv. Inorg. Chem.* **1995**, in press.

(50) (a) Absalon, M. J.; Stubbe, J.; Kozarich, J. W. *Biochemistry* **1995**, *34*, 2065−2075. (b) Absalon, M. J.; Wu, W.; Stubbe, J.; Kozarich, J. W. *Biochemistry* **1995**, *34*, 2076−2086.

(51) Povirk, L. F.; Han, Y.-H.; Steighner, R. J. *Biochemistry* **1989**, *28*, 5808−5814.

The proposed basis for specificity is more difficult to test experimentally, as it is clear that the pyrimidine moiety plays a key role not only in coordination of the metal[52] but also in the observed chemistry. However, the observation of a base-triple-like interaction from the minor groove is unusual and should allow modification of both the 5′-nucleotide and the pyrimidine of the CoBLM to effect a similar recognition pattern. Once again, quantitative structural studies can be carried out to test this prediction.

Summary. The studies reported herein delineate for the first time the role of both the 2-amino and N-3 of the guanine, 5′ to the pyrimidine cleavage site, in forming the basis for specificity involving the 4-amino group and N3 of the pyrimidine of the CoBLM A2 green. The linker plays a key role in appropriately positioning the bithiazole tail for binding by intercalation from the minor groove and thus providing the affinity for DNA. The use of CoBLM A2 green, a hydroperoxide analog of activated BLM, gives an unprecedented glimpse of the orientation of this group relative to the position on the DNA where chemistry occurs. Studies are in progress to test the generality of the observation with regard to both binding and specificity. We propose that CoBLM A2 green is an excellent model for activated BLM.

Acknowledgment. This research is supported by NIH Grant GM 34454 to J.S. and J.W.K. The NMR facility is supported by NIH Grant P41RR0095. We are grateful to J. Battiste, J. Williamson, and L. Stern for many helpful discussions. We are also grateful to S. Woodson for use of her computer equipment.

Supporting Information Available: Figures showing titration of d(CCAGGCCTGG) with CoBLM A2 green at 20 °C, the expanded NOESY spectrum of the base to H1′ region of strand 2 in the complex, and an overlay of the eight molecular dynamics structures (3 pages). This material is contained in many libraries on microfiche, immediately follows this article in the microfilm version of the journal, and can be ordered from the ACS; and can be downloaded from the Internet; see any current masthead page for ordering information and Internet access instructions.

JA952497W

(52) Loeb, K. E.; Zaleski, J. M.; Westre, T. E.; Guajardo, R. J.; Mascharak, P. K.; Hedman, B.; Hodgson, K. O.; Solomon, E. I. *J. Am. Chem. Soc.* **1995**, *117*, 4545−4561.